IOP Publishing Reports on Progress in Physics
Rep. Prog. Phys. 81 (2018) 016402 (12pp) https://doi.org/10.1088/1361-6633/aa8372

Review

# Emerging optical properties from the combination of simple optical effects

**Grant T England**[1] **and Joanna Aizenberg**[1,2,3]

[1] John A Paulson School of Engineering and Applied Sciences, Harvard University, Cambridge, MA, United States of America
[2] Wyss Institute for Biologically Inspired Engineering and Kavli Institute for Bionano Science and Technology, Harvard University, Cambridge, MA, United States of America
[3] Department of Chemistry and Chemical Biology, Harvard University, Cambridge, MA, United States of America

E-mail: jaiz@seas.harvard.edu

Received 3 March 2017, revised 12 June 2017
Accepted for publication 2 August 2017
Published 29 November 2017

Recommended Professor Masud Mansuripur

**Abstract**

Structural color arises from the patterning of geometric features or refractive indices of the constituent materials on the length-scale of visible light. Many different organisms have developed structurally colored materials as a means of creating multifunctional structures or displaying colors for which pigments are unavailable. By studying such organisms, scientists have developed artificial structurally colored materials that take advantage of the hierarchical geometries, frequently employed for structural coloration in nature. These geometries can be combined with absorbers—a strategy also found in many natural organisms—to reduce the effects of fabrication imperfections. Furthermore, artificial structures can incorporate materials that are not available to nature—in the form of plasmonic nanoparticles or metal layers—leading to a host of novel color effects. Here, we explore recent research involving the combination of different geometries and materials to enhance the structural color effect or to create entirely new effects, which cannot be observed otherwise.

Keywords: structural color, Bragg stack, bioinspiration, diffraction grating, hierarchy, plasmonics, DBR

(Some figures may appear in colour only in the online journal)

## 1. Introduction

Structurally colored materials (SCMs) are prized for the absence of photobleaching in their long-term performance and wide range of optical properties and special color effects, such as iridescence or environmentally-induced color change, not obtainable in bulk materials and in standard pigments [1–4]. Color from dyes and pigments is generated by the excitation of electron/hole pairs via the absorption of photons with specific wavelengths. There is a finite probability of electron or hole capture, leading to the creation of chemically reactive free radicals, which can react with the dye to change its chemical structure. This irreversible chemical change in the dye's molecular structure results in the color fading over time as more and more of the dye molecules are photo-bleached. Therefore, improvement of dye longevity is an active area of research [5–7]. SCMs are naturally immune to the photobleaching-induced color fading because their coloration comes from light interference effects within the structure. With the recent focus on environmental concerns related to dyes and pigments, the ability to utilize inert materials for the creation of color is more important than ever [8].

 

SCMs are broadly present in nature and through millions of years of evolution organisms have optimized their color-producing features by utilizing SCMs alone, pigments, or combinations of the two to achieve their desired appearance [9]. Using such organisms as inspiration, scientists have learned how to create and optimize SCMs for a variety of purposes [10]. The use of bio-inspired, rather than bio-mimetic [11], approaches in this field have yielded materials, which capture the essence of the color-producing elements in natural organisms by distilling the structures down to their key components: (i) order/disorder, (ii) hierarchy, and (iii) absorption/scattering.

SCMs can largely be described using the terminology of photonic crystals—periodic structures in 1-, 2-, or 3-dimensions that modify the propagation of light [12]. The use of order and disorder in photonic crystals allows for control over the amount of angular variation or color travel, with more disordered materials having less angular dependence of their reflected color due to the lack of coherent crystal planes within the photonic crystal. Scientists have gained a fundamental understanding of the interrelationship of structural arrangements and the resulting coloration of a material and have used this understanding to fabricate structured materials with controlled order or disorder at the nanometer length scales [13].

Hierarchy is a common theme in biological materials, whether as a necessity for multifunctional materials or a consequence of self-assembly [14]. For SCMs, this hierarchy is the simplest method by which to obtain multiple optical effects from the same structure. Using combinations of self-assembly and top-down fabrication methods, scientists have been able to create hierarchical nanostructures for a variety of applications [15].

Absorption and scattering can also be used to influence the color produced by SCMs. Scattering within an imperfect SCM or reflections from surfaces outside of the SCM can lead to the desaturation of the structural color, leading to a whitish appearance. If saturated colors are desired, absorbers can be used to mitigate the color desaturation, which is caused by scattering, by absorbing some of the broadband scattered light. On the other hand, strong scattering can itself lead to enhanced color saturation. For example, when there is a surface external to the SCM that is affecting its color, a strong scattering layer can be used to reduce the coherence of the reflecting surface.

It is important to realize that nature has developed its panoply of SCMs using a very limited set of materials within extremely constrained systems. Organisms must, naturally, rely on biological components and bottom-up self-assembly to create any material; for SCMs in nature therefore, the most restricting constraint is the lack of high refractive index materials (some of the highest are guanine, $n = 1.83$ and chitin/keratin $n = 1.54$) [16], which limits the obtainable index contrast required for high-performance photonic structures. Tools and materials developed in the laboratory can be used to expand the diversity of SCMs leading to a variety of possibilities that cannot be observed in nature. By using plasmonic materials and high-index dielectrics, which are typically unavailable for biological organisms, the physical size of SCMs can be greatly reduced. In addition, the large imaginary portion of the complex refractive index of these materials causes the phase change upon reflection from their surface to be anomalous (different from the 0 or $\pi$ phase change from non-absorbing materials). This anomalous phase-shift can lead to many types of SCMs, as well as allow for a great reduction in the thickness required for thin-film photonic structures.

This review discusses three techniques to create or enhance SCMs: (1) hierarchical structuration to take advantage of the optical properties of multiple structural elements, (2) absorption for color purification of SCMs or to cause asymmetric effects due to the anomalous phase change upon reflection from an absorbing layer, and (3) introduction of plasmonic moieties to reduce the physical size of SCMs in order to create materials that do not exist in nature. All of these techniques use engineered structures to combine relatively simple optical effects and achieve complex optical properties.

## 2. Hierarchy and disorder

Biology has developed a host of SCMs, including diffraction gratings, multilayers, and 3D photonic crystals [9, 16]. A particular strength of these biological SCMs is their use of hierarchy to generate optical effects that would not be possible using idealized models one might find in a standard optics textbook. For example, a common method to reduce the angle-dependence of structural color is to introduce disorder into a 3D photonic crystal such that the local order is strong enough to create a structural color, but the long-range order is weak [17, 18]. Thus, many different photonic crystal 'grains' of slightly different orientations are observed simultaneously and their individual angle-dependence is averaged leaving only the primary peak to be easily observed. Many scientists utilize this effect to generate structural color pigments that appear uniform for various incidence and observation angle combinations [17, 19–24]. Since disorder is desired for this angle-independent effect, dynamic SCMs can be created by embedding colloidal particles in a flexible material such that the average difference between particles can be tuned by an external force [25–27]. A thorough discussion of the optical properties of disordered systems can be found in the review by Galisteo-Lopez *et al* [13]. In addition, hierarchical structuration can be used as a diffusive component, and therefore reduce the angular dependence of a structural color. For example, many species of butterfly, including those of the famous *Morpho* genus, reduce color iridescence due to combinations of diffraction gratings and multilayer structures [28–30].

A recurring motif of hierarchical SCMs in nature is the combination of a diffraction grating with another optical element; a wide range of possibilities for such a combination is depicted in figure 1. Often, the superposition of a diffraction grating with another optical element, such as 3D photonic crystal or a multilayer, as is the case for *Morpho rhetenor*, is used to give a wider angular distribution to the visibility of a structural color (figure 1(a)) [31–33]. However, several other interesting effects can be achieved by creating hierarchical structural color materials of different types. A thin film in conjunction with a diffraction grating can produce predictable

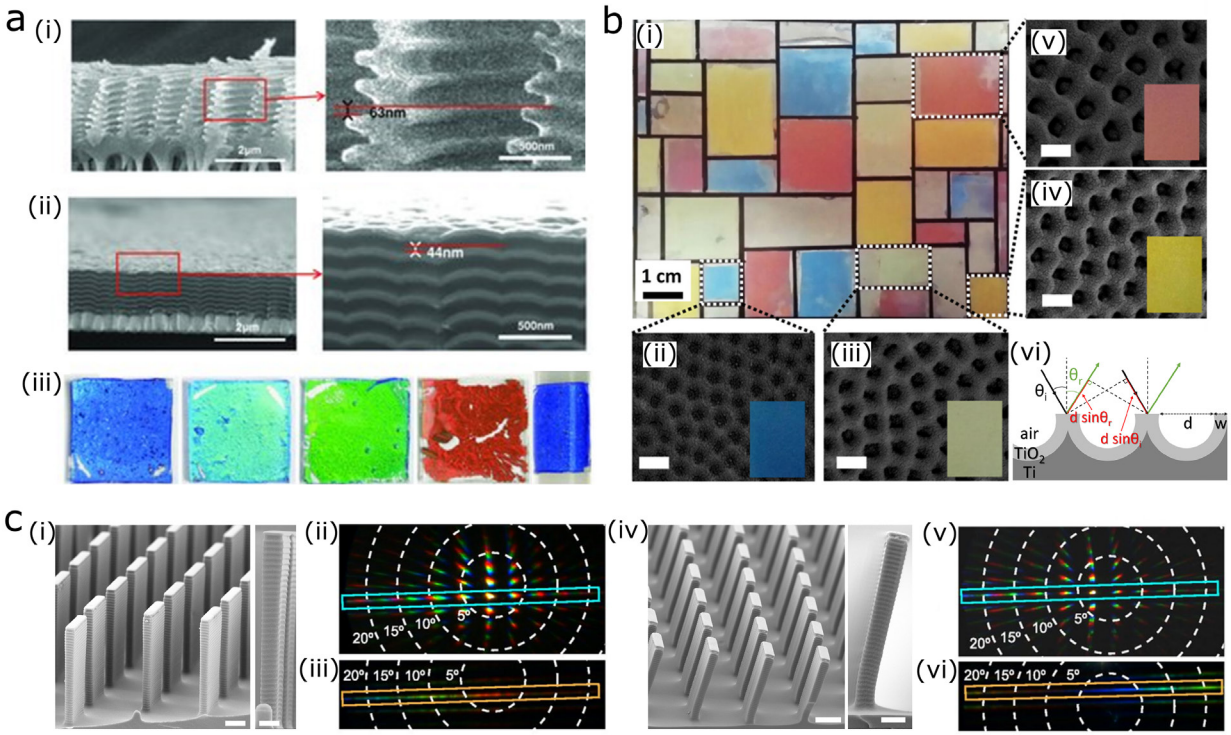


**Figure 1.** Combination of diffraction gratings with other structural color elements. (a) Diffraction grating + multilayer. Structural comparison between butterflies and fabricated angle-insensitive structural color films. [31] John Wiley & Sons. Copyright © 2012 WILEY-VCH Verlag GmbH & Co. KGaA, Weinheim. (i) (Left) cross-sectional SEM image of the multilayered ridges on the dorsal ground scale of a *Morpho Didius* butterfly. (Right) a close-up view of the ridges, showing a vertical offset of 63 nm between two neighboring ridges, taken from the area outlined in red. (ii) (Left) cross-sectional SEM image of the deposited multilayer thin film. The bright layers are $SiO_2$ and the dark layers are $TiO_2$. A Cr-covered monolayer of silica microspheres is located at the bottom of the multilayer structure, causing a column-like structure in the multilayer. (Right) a close-up view of the multilayer, showing a vertical offset of 44 nm between neighboring columns (similar to the ridge offset in (i)), taken from the area outlined in red. (iii) Images of fabricated films. Various colors ranging from deep blue through green to coppery red realized by controlling the layer thicknesses. The far right image shows the deep blue reflector wrapped around a rod with a diameter of 1 cm; note that the color appears the same throughout, even though the reflector is bent, and thus presents a viewing angle that varies from 0 to 90°. (b) Diffraction grating + thin film structural color painting using thin-film structured gratings in Littrow configuration. Reprinted with permission from [34]. Copyright (2016) American Chemical Society. (i) Centimeter-scale reproduction of a Mondrian painting titled 'composition with color planes and gray lines'. (ii)–(v) SEM images of selected areas, which illustrate different diameters and uniform alignment of the nanobowls. White scale bars are 200 nm. (vi) Ray diagram depicting light reflection from $TiO_2$ nanobowls of diameter $d$ and wall thickness $w$. $\theta_i$ and $\theta_r$ are the angle of incidence and reflection, respectively. (c) Diffraction grating + diffraction grating. Reverse color-order diffraction grating based on the *Pierella luna* butterfly. Reproduced with permission from [35]. © 2017 National Academy of Sciences. (i) (Left) SEM of an array of scalloped microplates. Scale bar, 5 $\mu$m. (Right) SEM of an individual plate with regular scallops clearly visible. Scale bar, 2 $\mu$m. (ii) Diffraction pattern caused by the periodic ensemble of microplates for 45° light incidence. A choice of propagation angles is visualized by the white dashed lines. (iii) Diffraction pattern resulting from the scallops on individual plates. (iv)–(vii) Same as (i)–(iii), for tilted gratings.

structural colors, which can be used as a mechanism for 'printing' structural color (figure 1(b)) [34]. Another option is to combine one diffraction grating with an orthogonally oriented diffraction grating. This can lead to a reverse color-order diffraction pattern wherein the color shifts from red to blue as the observation angle is increased, instead of the typical blue-to-red color order, an effect that can also be found in nature on the wings of the male butterfly *Pierella luna* (figure 1(c)) [35, 36]. In these examples, the combination of a diffracting grating with another optical structure is used to achieve novel optical properties.

Other types of geometries can be combined hierarchically to generate complex optical effects. Combining a multilayer with a retroreflector in different configurations can give rise to spatially modulated reflection colors as exemplified in the butterfly *Papilio blumei* [37] (figure 2(a)(i)–(iv)). By slightly modifying the organization of the structural elements—namely by placing the multilayer above the retroreflecting concavities rather than depositing it conformally on top of them—a different effect can be created wherein the reflected color of the multilayer and its transmission color can both be observed in reflection mode, albeit with orthogonal polarizations [37] (figure 2(a)(v)). Meanwhile, diffraction gratings are also frequently used to increase the light transfer efficiency into or out of light-generating or absorbing structures [38–46] as gratings promote out-coupling of light that would otherwise be trapped by total internal reflection modes. As seen in figure 2(b), the addition of gratings can therefore lead to brighter light emitting diodes (LEDs) [47, 48]. Moreover, a multilayer Bragg stack can be fabricated using a porous 3D photonic crystal as one of the alternating materials to allow for hygroscopic color change as is the case in Longhorn Beetles [49].

In all the cases discussed above, hierarchy is used to enrich the optical properties of an SCM. These examples only rely on

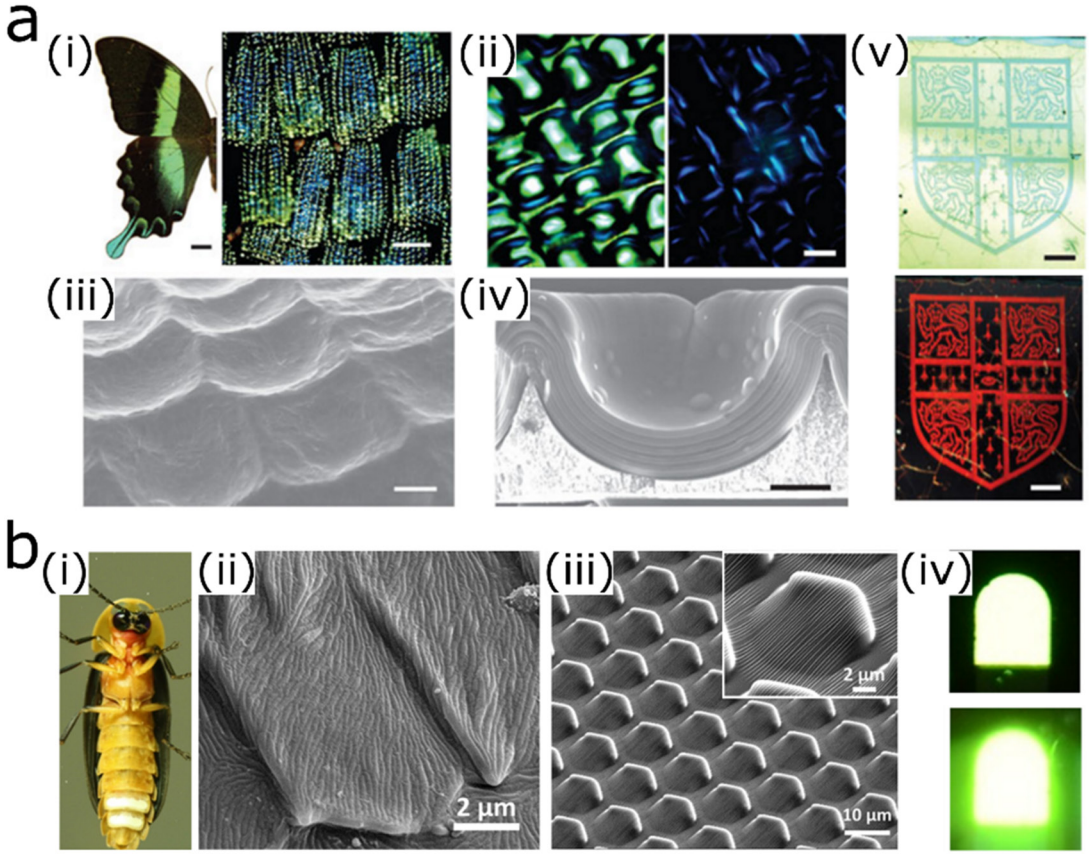


**Figure 2.** Arrayed hierarchical optical structures. (a) Multilayer + retroreflector for polarization-dependent color. Reprinted by permission from Macmillan Publishers Ltd: Nature Nanotechnology [37], Copyright (2010). (i) The bright green wings of the *P. blumei* butterfly result from the mixing of the different colors that are reflected from different regions of the scales found on the wings of these butterflies (scale bars: left, 1 cm; right, 100 $\mu$m). (ii) and (iii) Optical micrographs ((ii), scale bar: 5 $\mu$m) and SEM images ((iii), scale bar: 2 $\mu$m) showing that the surface of a wing scale is covered with concavities (diameter $\approx$ 5–10 $\mu$m) that are arranged in ordered lines along the scale. These concavities are cladded with a multilayer that reflects yellow–green light at their centers and blue at their edges ((ii), left). By observing the scales in an optical microscope with crossed polarizers, the yellow–green light is extinguished, but the blue light can still be detected along four segments of each edge ((ii), right). (iv) SEM of a fabricated concavity covered by a conformal multilayer stack of 11 alternating layers of titania and alumina (scale bar: 1 $\mu$m). (v) Samples viewed in direct specular reflection (top) and in retro-reflection (bottom) (scale bars 5 mm), show a striking change in color from blue to red, for a different sample with the multilayer above the concavity. (b) Combination of hierarchical structures with an LED to enhance out-coupling of light based on the microstructures found in firefly lantern scales. Reprinted with permission from [48]. Copyright (2016) American Chemical Society. (i) An optical image of a male firefly (*Pyrocoelia rufa*). (ii) SEM of the male firefly lantern cuticle. (iii) Perspective SEM of the hierarchical structures designed based on the structures in (ii). (Inset: magnified view). (iv) Photographs of OLEDs in operation without (top) and with (bottom) structured surfaces.

the combination of different morphologies of purely dielectric materials to generate interesting and useful structures. An even greater variety of effects can be achieved by introducing optically active elements, such as absorbers, into SCMs.

## 3. Absorption

Typically, absorption is added to a SCM in order to reduce the desaturation of color that originates from nonspecific scattering (i.e. broadband scattering resulting from inhomogeneities in the material). Scattering is typically stronger for shorter wavelengths; for the Rayleigh limit of Mie scattering (scatter size $\ll \lambda$), the scattering cross-section is proportional to $\lambda^{-4}$, however, it should be noted that the enhanced blue scattering in photonic glasses is due to an ensemble effect [22]. So, this desaturation effect is most noticeable when a structural blue color is being created, as is the case for the brilliant blue Steller's jay bird, which appears pure white (due to scattering) when the bird has no melanin in its plumage [50]. In real-world structures (whether biological or man-made), there are many causes of such nonspecific scattering, such as inevitable deviations from perfect periodicity and the presence of unintended surface roughness. An absorbing moiety (whether a dye or an absorbing plasmonic nanoparticle) dispersed homogeneously throughout the SCM can greatly reduce the desaturation effects of this nonspecific scattering. Even for broadband absorbers such as carbon black, the color purity of the material can be improved, as the intensity of the structural color peak relative to the background will be increased [23, 51–56]. This approach is general and will improve the color saturation for color produced by multilayers or 3D photonic crystals, provided the doping level of the absorbing particles is correctly optimized (this optimization process will vary depending on the type of SCM being created and the type of

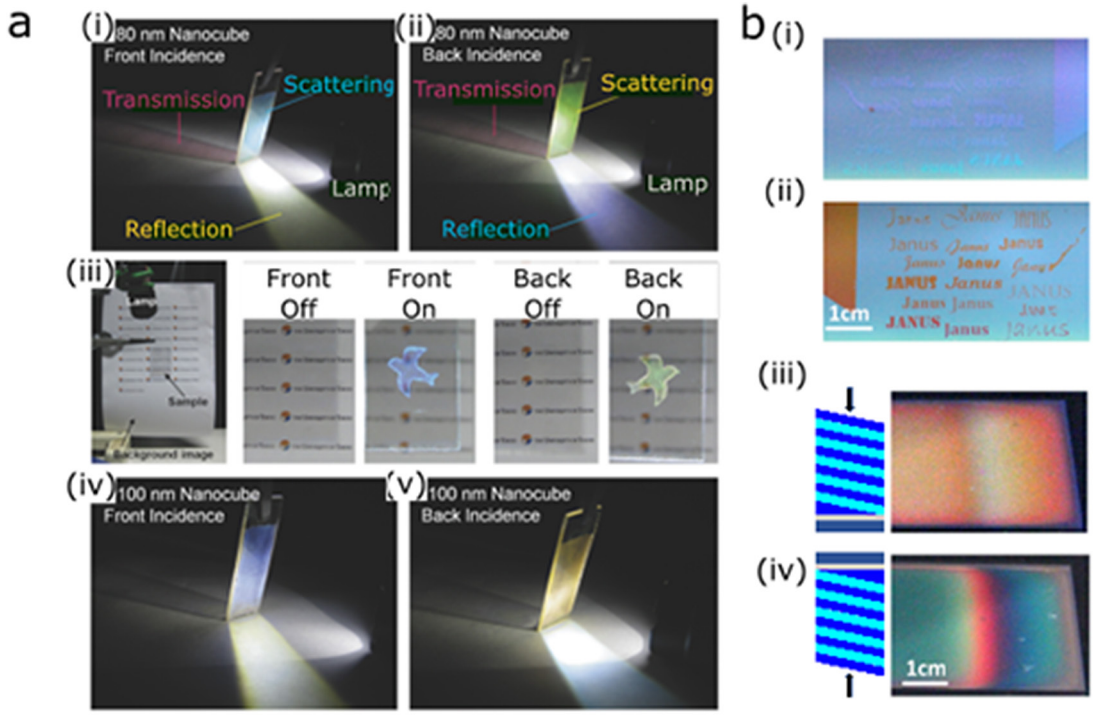


**Figure 3.** Asymmetric optical effects achieved by adding structured absorption to SCMs. (a) Optical behaviors of Ag nanocubes on thin $TiO_2$-coated glass plates. From [60] John Wiley & Sons. © 2015 WILEY-VCH Verlag GmbH & Co. KGaA, Weinheim. (i)–(v) Asymmetric color routing for the front (i), (iv) and back (ii), (v) incidence. (iii) Dichromatic scattering. A bird image drawn by Ag nanocubes is almost invisible under ambient light both from the front and back side. The image is clearly visible both from the front and back side when the sample is illuminated by a Xe lamp from the side of the observer. (b) Viewing direction-dependent optical effects from Janus coatings using a thin metal film as the absorbing element. From [61] John Wiley & Sons. © 2017 WILEY-VCH Verlag GmbH & Co. KGaA, Weinheim. (i) and (ii) Partially invisible Janus color patterns: (i) photograph of the coating side surface of a micro-patterned asymmetric structural color stack of SiN and $SiO_2$ with a thin film of patterned chromium designed to match colors of the features and the background from the coating side and thus hide the pattern. (ii) Photograph of the substrate side surface of the sample in (i) showing high contrast between the color in the regions containing chromium and those containing only the Bragg stack. (iii) Photograph of a structure of SiN/$SiO_2$ with a gradient-thickness layer of SiN and a thin film of chromium, showing a near solid orange color when viewed from the coating side. (iv) Sample in (iii) photographed from the substrate side, revealing a rainbow pattern in the region of the thickness gradient.

absorber being used). For situations in which the desired color is known *a priori*, a specific absorber can be chosen such that its absorption spectrum does not overlap with the structural color peak; however, it can be challenging to find an absorber whose spectrum precisely corresponds to the desired color of the SCM [57–59].

When the absorbing moieties are localized at defined areas within the SCM instead of distributed homogenously throughout it, more complicated optical effects can arise beyond the reduction of nonspecific scattering. Specifically, drastically different colors can be achieved by using different illumination and observation conditions. Asymmetric reflection (and absorption) can be observed by defining an absorbing layer on a transparent substrate that is coated with at least one layer of a dielectric thin film (one which would give rise to structural color even in the absence of an absorber). The effect can be observed with a range of absorbing layers, for example plasmonic nanoparticles [60–62], structured plasmonic absorbers such as metal hole arrays [63], or simply thin metal films [61]. A fully dielectric Bragg stack without absorbers will appear identical regardless of which side is being observed.

As shown in figure 3, the addition of an absorbing layer leads to a different observed color when viewing from the top of the sample as compared to the bottom. This geometry allows for the structure to be partially transparent; therefore, the structure is not equivalent to a substrate coated on either side with a pigment (which would also display different colors depending on which side is being viewed) and a third color can be observed when viewing the sample in transmission mode. Due to conservation of energy, the difference in reflected color must also manifest itself in a difference in the absorption or scattering between the different sides of the structure since the transmission must be the same due to reciprocity. The article by Jalas *et al* [64] describes the consequences of this reciprocity with regards to the creation of optical isolators quite thoroughly; briefly, if the structures do not break Lorentz reciprocity, which states that the material must behave identically if we reverse the location of the light source and the detector, the transmission must be identical for both directions. These three different color effects are clearly visible in figure 3(a). This effect has been used to create asymmetric absorption materials for potential applications in photovoltaics [63, 65], facile glass structural coloration [66], and plasmonic color routing [60]. Another interesting feature is that multilayer Bragg stacks can be used to further tune the reflected colors from either side of the SCM and allow for viewing-direction-dependent camouflage of a photolithographically designed pattern (figure 3(b)(i)). Moreover, the introduction of a

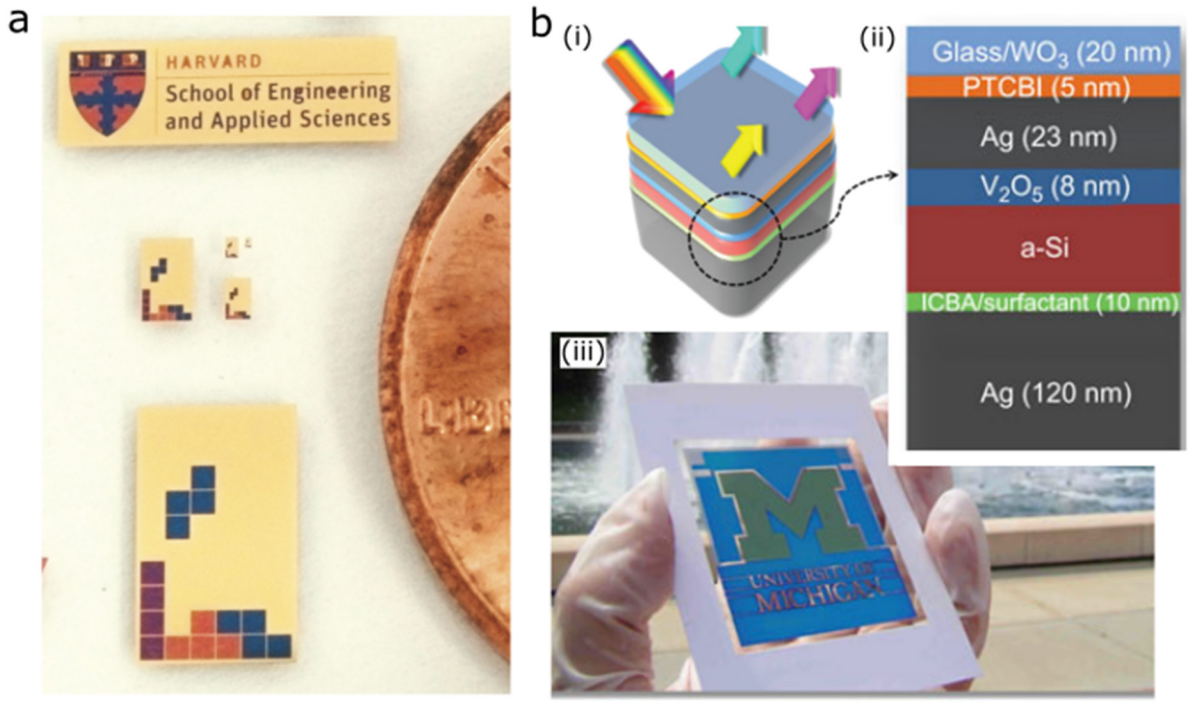


**Figure 4.** Ultra-thin SCMs. (a) Germanium thin film colored film. Reprinted by permission from Macmillan Publishers Ltd: Nature Materials [69], Copyright (2013). Five steps of photolithography with alignment are used to selectively deposit an optically thick layer of Au on a glass slide, followed by Ge layers of either 7, 11, 15 or 25 nm. This yields light pink, purple, dark blue and light blue colors, respectively. (b) Colored ultra-thin photovoltaic. Reprinted by permission from Macmillan Publishers Ltd: Nature [76], Copyright (2014). (i) Schematic of the device structure. (ii) The cathode comprises a thick Ag layer and an organic layer, and a dielectric-metal structure is used for the anode. Between the two electrodes is an ultrathin amorphous silicon (a-Si) layer. (iii) A university logo, consisting of green and blue colors, is successfully realized with the generation of electric power.

gradient-thickness layer into a Bragg stack designed with its peak in the center of the visible spectrum, can allow for a sample that appears nearly monochromatic from one side, while allowing for a smooth color gamut to be viewed from the other side [61] (figure 3(b)).

This type of coloration methodology can also be used on non-transparent substrates for a variety of color applications as shown in figure 4. Since these materials include a thin absorbing layer, the anomalous reflection from this layer, which has a phase shift that is different from 0 or $\pi$, leads to vastly different conditions for destructive and constructive interference. Thus, interference can be achieved using dielectric/absorber thicknesses much smaller than the wavelength [67], as compared to typical thin film coatings, which have their first order constructive interference peak at half of the optical thickness of the film. Ultra-thin structural color coatings [68–72] such as the one highlighted in figure 4(a), or ultra-thin absorbing coatings (structural black) [67, 73–75] can be used to color a material with a much thinner coating than would be possible with a standard Bragg stack. This method has even been applied to solar cells to color the solar cells by varying the thickness of a dielectric within the photovoltaic architecture (figure 4(b)) [76, 77].

Until this point, we have shown that the addition of absorbing layers can be applied to increase the color saturation of a SCM and that by structuring the absorption within the SCM, ultra-thin colored materials and asymmetric reflection/absorption materials can be created. These examples of patterned absorption, rely on tight confinement of the absorber in one dimension only (although large-scale patterning of this confinement is also possible). With the addition of patterning the absorber in two and three dimensions on smaller length scales, we enter the realm of plasmonics and allow for the creation of a host of colored materials on a different length scale than those previously reported and utilizing a different design paradigm.

If metal films are used instead of absorbing particles, the absorption begins to affect the resonance of the SCM more directly due to the typically high index of refraction of metals as compared to the effective index of refraction of a dielectric film containing metal nanoparticles. In this way, color filters can be made much thinner than conventional dielectric Bragg stacks by using metal–insulator–metal structures [78–83]. When there are a large number of metal layers separated by dielectrics, and the layers are sufficiently thin, such a material constitutes one type of a hyperbolic metamaterial (a material having hyperbolic or indefinite dispersion) [84] and can be used for applications in superlensing, negative index of refraction, and sensing [85].

## 4. Plasmonics

In the previous section, the addition of plasmonic absorbers was discussed as a method for either providing wavelength-selective absorption to improve the color saturation of an SCM or a way to tailor the complex refractive index of an absorbing layer to achieve asymmetric reflection/absorption properties in a multilayer architecture. In addition to these applications, plasmonic absorbers can be designed or patterned to allow for polarization- or angle-dependent color effects enabled by the

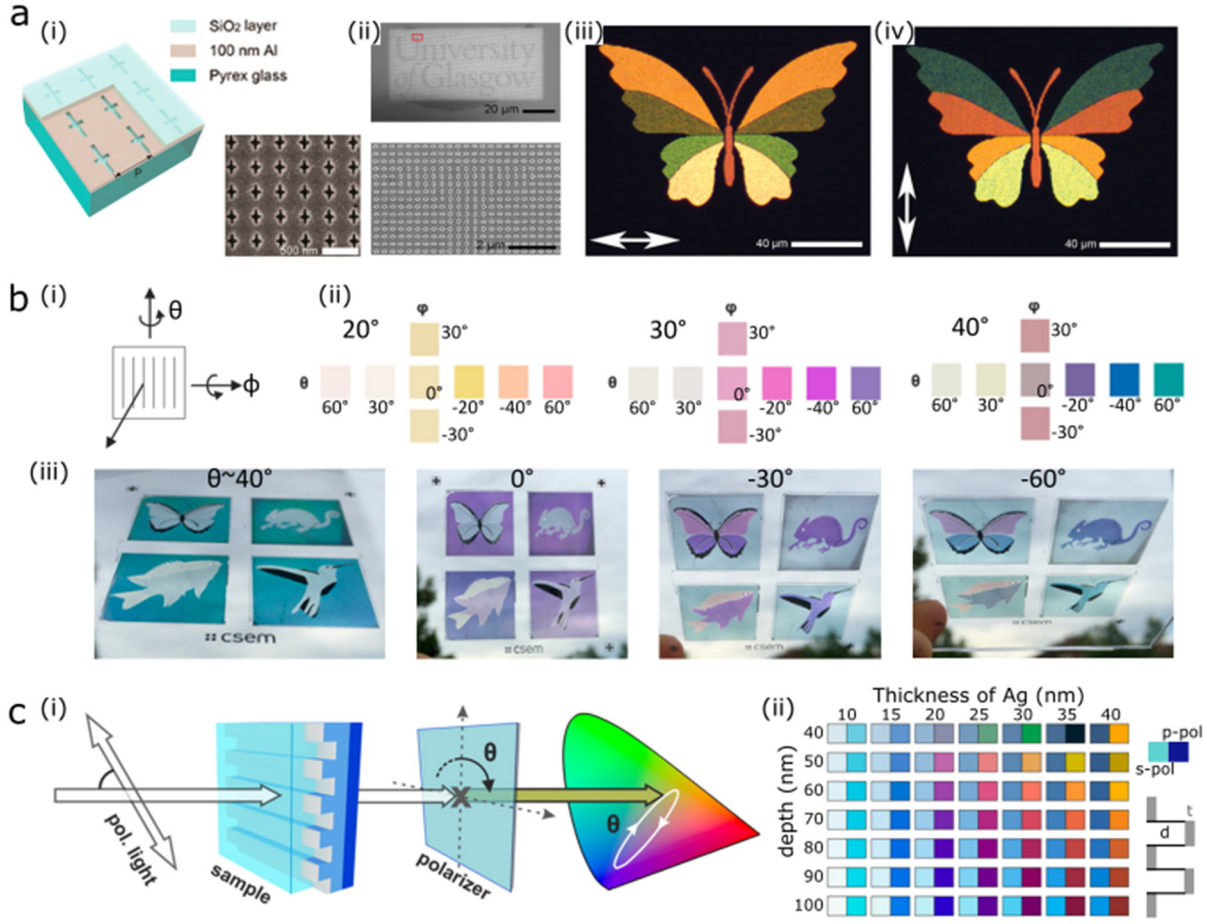


**Figure 5.** Polarization- and angle-dependent colors created using patterned plasmonic absorbers. (a) Polarization-dependent structural colors based on t-shaped resonators. Reprinted with permission from [86]. Copyright (2016) American Chemical Society. (i) (Left) schematics showing aperture geometry and arrangement and (right) SEM of a typical pixel array. Scale bar 500 nm. (ii) SEM image with enlarged view shows the top right part of letter *U*. The pixels in letter sections are rotated through 90° with respect to those in the background region. Scale bars, 20 $\mu$m and 2 $\mu$m. (iii) and (iv) Microscope images of a butterfly with switchable wing panel colors due to the electric-field of the incident light being polarized along the *x* and *y*-axes, respectively (the arrows display the oscillation direction of the electric-field). Scale bars 40 $\mu$m. (b) Asymmetric color behavior of asymmetric aluminum-coated gratings. Reprinted with permission from [87]. Copyright (2015) American Chemical Society. (i) Sketch defining viewing angles $\theta$ and $\varphi$. (ii) Measured colors of the samples characterized for different evaporation angles (bold) and different viewing angles $\theta$ and $\varphi$ defined in sketch. Colors mainly appear at negative angles $\theta$. (iii) Glass substrates with 4 different sample areas (2 cm $\times$ 2 cm) created by the evaporation angles 20°, 30° and 40°. Photographs were taken in front of a cloudy sky and with unpolarized light. (c) Four-fold color filter. Reprinted with permission from [88]. Copyright (2016) American Chemical Society. (i) Schematic of the experimental setup showing (form left to right) the input linearly-polarized light, the plasmonic phase-retarding sample, the analyzing polarizer, the CIE *x*-*y* color space with a closed loop representing the obtainable colors for the sample. (ii) Simulated color map of s-pol and p-pol colors for varying depth and silver thickness. The illustrations qualitatively indicate the arrangements. The color palette displays the computed transmission color.

difference in efficiency with which light can couple into the absorbing plasmonic modes depending on its polarization and incidence angle.

Several studies have probed the use of plasmonic absorbers for polarization and angle-dependent colors. Plasmonic absorbers featuring asymmetric geometries can be used to tune the color for two orthogonal resonances nearly independently [86] (figure 5(a)). Angular asymmetry in the color produced by a grating can be achieved by coating the grating asymmetrically with a plasmonic metal [87] (figure 5(b)). Similarly, by introducing an analyzing polarizer into the setup, color filters, which produce several different colors depending on the polarization of the incident illumination and the relative angle of the analyzing polarizer, can be created [88] (figure 5(c)). In addition, metal nanowire arrays with different periodicities [89–92] and pillar-based gratings (sometimes referred to as vertical nanowires) [93–96] have also been used to create polarization-dependent color filters. Such polarization and angle-dependent structures can be used as filters or color routers in optical experiments or as security materials for anti-counterfeiting purposes.

As discussed previously, by incorporating hierarchical structures and absorbing materials, the photonic properties of SCMs can be improved, while the number of repeating units, and thus their physical size, can remain constant or even be reduced. The dimensions of these structures can be reduced even further by creating metasurfaces, the 2D analog of metamaterials [97]. These can be designed to produce a variety of optical effects with extremely thin photonic devices. Several review articles have already been written on this topic [98–100]. Here, we will focus on the use of metasurfaces to achieve color effects similar to those discussed above.

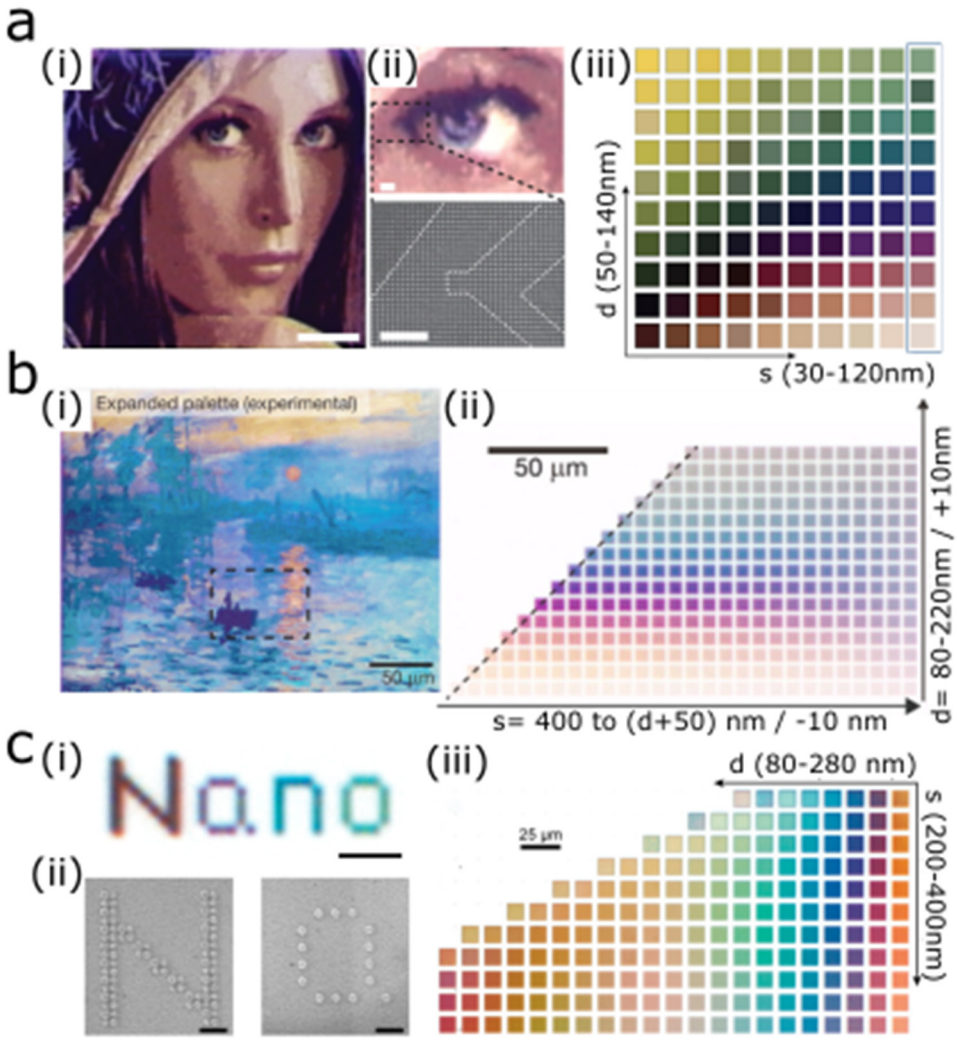


**Figure 6.** Improvements in color palette available for plasmonic printing. (a) Gold-coated pillar arrays with varying spacing and diameter. Reprinted by permission from Macmillan Publishers Ltd: Nature Nanotechnology [101], Copyright (2012). © Playboy Enterprises, Inc. (i) Optical micrographs of the Lena image after metal deposition. (ii) Optical micrograph of an enlarged region of the image (top) with SEM image of the indicated region (bottom) for clarity, the individual regions of similarly sized disks are separated by the dotted lines. Each pixel consists of a 2 × 2 array of disks with a pitch of 250 nm. (iii) Full color palette obtainable with this method showing similar colors from bottom left to top right, indicating that areas with similar fill factors produce areas with similar colors. Squares are 12 $\mu$m × 12 $\mu$m. The highlighted column was used to produce the image in (a)((i) and (ii). (b) Aluminum-coated pillar arrays with varying space and diameter. Reprinted with permission from [107]. Copyright (2014) American Chemical Society. (i) Realistic reproduction of Monet's 'impression, sunrise' using an expanded palette of colors. (ii) Spacing color palette with both size variations ($d$ = 80–220 nm) and spacing variations ($s = d$ + 50–400 nm) among four nanodisks within an 800 × 800 nm pixel, at a step size of 10 and 20 nm, respectively. Optical images were normalized to a white background. (c) Aluminum nano-disks on aluminum oxide coated aluminum with varying spacing and diameter. Reprinted with permission from [110]. Copyright (2016) American Chemical Society. (i) Optical micrograph of the subwavelength-pixel 'nano' letters in color. The patterns are composed of dark color and colored pixels (violet, $d$ = 100 nm; blue, $d$ = 120 nm; green, $d$ = 140 nm). Each single pixel is a 300 nm × 300 nm square. The images were obtained through an objective of 150 × and 0.9 NA. Scale bar, 2 $\mu$m. (ii) SEM images of enlarged regions of '*N*' and '*a*'. Scale bar, 500 nm. (iii) Optical image of nanodisk arrays with varying diameters $d$ from 80 to 280 nm in 10 nm increments and periods $P$ from 200 to 400 nm in 20 nm increments. The image was obtained with a 20 × objective (NA = 0.45) under unpolarized white light illumination.

Metasurfaces can be used to create the highest resolution color images in existence, which has potential in high density data storage, anti-counterfeiting, and color filtering for display technologies. Taking advantage of the high physical confinement allowed by plasmonic structures and the utility of modern fabrication methods, specific plasmonic absorbers can be fabricated with increased precision to allow for full color images to be achieved on unprecedented size scales. Nanoscale arrays of pillars, holes, or pillar/hole combinations coated with films of plasmonic metals can feature high quality factor resonances, generate different colors in pixels as small as 250 × 250 nanometers, and allow for 100 000 dpi printing as shown in figure 6(a) [101]. Many groups have developed and expanded this field by increasing the scalability of the technique [102], or creating angle-independent structural color on a similar length scale [103], or even creating the prototypical full-color electronic-ink displays [104].

More recently, there has been a growing trend to move away from expensive noble metals [105, 106] as the plasmonic material and shift to using other materials, which have

favorable plasmonic properties at visible wavelengths and give a more neutral white color for the back-reflected light. Using aluminum, for example, the color palette available for metal-coated photoresist post arrays has been expanded (figure 6(b)) [107–109]. Additional geometries of aluminum nano-disk or nano-hole metal–insulator–metal structures (figure 6(c)) [110, 111] allow for the use of different fabrication technologies (such as nanoimprint or focused ion beam lithography) to create the structures, with similar achievable colors and resolutions. These techniques often employ soft lithography to replicate an electron-beam lithographically generated master so that many samples can be created rapidly. Others rely on colloidal lithography [112–114] to generate resonators of the desired shape and periodicity, but this technique does not allow for high-resolution patterning of the resultant structures [115–119]. Directed self-assembly of pre-synthesized nanoparticles can be used to allow for high resolution and polarization-dependent color [120], but this technique requires a different photolithographic step for every type of nanoparticle (and therefore basis color) being deposited. A more realistic method for generating a large number of photonic/plasmonic nanostructures is to use nanoimprint lithography as discussed in a recent review [121]. This type of structural color printing has been further pushed towards display applications by integrating the plasmonic pixels with a tunable liquid crystal to enable a method to actively change the color of a plasmonic image [122, 123] and by fabricating the structures on a stretchable substrate to allow for dynamic tuning of the spacing between the plasmonic elements [124].

Plasmonic absorbers can be used to enrich SCMs in a variety of ways. By designing asymmetric plasmonic absorbers, polarization- and angle-dependent color filters can be realized. By increasing the dimensionality of this patterning further, metasurfaces with all kinds of optical properties can be fabricated. The field of plasmonic printing allows for the highest resolution color images possible to be created, although the complexity of the fabrication does not yet allow for large numbers or unique samples or dynamic display technologies.

## 5. Conclusions

In this review, we have discussed several different methods for creating novel SCMs: (1) hierarchical structuration and disorder can be used to generate optical effects that are unobtainable with simple geometries or to mitigate the iridescence of SCMs, (2) absorption can be used either to purify the spectrum of an SCM or to expand the SCM's behavior due to the plasmonic or optical phase-change properties of the defined absorbing layer, and (3) plasmonic materials can be used to create much smaller photonic architectures by taking advantage of the extremely high confinement and purity of the available photonic modes in the structures. The toolkit discussed in this review has been built up from combinations of classical SCMs and includes the addition of absorbers as well as patterned plasmonic materials. These tools have led to the discovery of new types of SCMs and have allowed for the improvement and extension of their optical performance. Decades or centuries after understanding the fundamentals of the individual optical elements, the field of structural coloration is still very active and the combination of simple and well understood optical elements continues to yield materials with surprising optical effects. The discovery of the intricate nature of light matter interactions at different length scales naturally precedes applications, but it is clear that such effects will be useful in diverse fields of technologies, including imaging, display technologies, photovoltaics, colorimetric sensing, high density optical storage, and security printing will be improved by their development.

## Acknowledgments

This work was supported by the NSF Designing Materials to Revolutionize and Engineer our Future program (DMR 1533985).

## References

[1] Kinoshita S, Yoshioka S and Miyazaki J 2008 Physics of structural colors *Rep. Prog. Phys.* **71** 076401
[2] Pfaff G and Reynders P 1999 Angle-dependent optical effects deriving from submicron structures of films and pigments *Chem. Rev.* **99** 1963–82
[3] Yetisen A K *et al* 2016 Art on the nanoscale and beyond *Adv Mater* **28** 1724–42
[4] Park C, Koh K and Jeong U 2015 Structural color painting by rubbing particle powder *Sci. Rep.* **5** 8340
[5] George J, Gireesh V S, Ninan G and Krishnan Nair S 2015 Modification of $TiO_2$ surface for improved light fastness *Int. J. Ind. Chem.* **6** 133–41
[6] Kim T and Chae Y 2014 Synthesis and application of novel high light fastness red dyes for ultra high molecular weight polyethylene fibers *Fibers Polym.* **15** 248–53
[7] Gajadhur M and Łuszczyńska A 2017 Influence of pearlescent pigments on light-fastness of water-based flexographic inks *Dyes Pigm.* **138** 119–28
[8] Shahid M, Shahid ul I and Mohammad F 2013 Recent advancements in natural dye applications: a review *J. Clean. Prod.* **53** 310–31
[9] Vukusic P and Sambles J R 2003 Photonic structures in biology *Nature* **424** 852–5
[10] Zhu Y, Zhang W and Zhang D 2017 Fabrication of sensor materials inspired by butterfly wings *Adv. Mater. Technol.* **2** 1600209
[11] Kraus T, Brodoceanu D, Pazos-Perez N and Fery A 2013 Colloidal surface assemblies: nanotechnology meets bioinspiration *Adv. Funct. Mater.* **23** 4529–41
[12] Joannopoulos J D, Johnson S G, Winn J N and Meade R D 2008 *Photonic Crystals: Molding the Flow of Light* (Princeton, NJ: Princeton University Press)
[13] Galisteo-Lopez J F *et al* 2011 Self-assembled photonic structures *Adv. Mater.* **23** 30–69
[14] Schacher F H, Rupar P A and Manners I 2012 Functional block copolymers: nanostructured materials with emerging applications *Angew. Chem., Int. Ed. Engl.* **51** 7898–921
[15] Vogel N, Retsch M, Fustin C A, Del Campo A and Jonas U 2015 Advances in colloidal assembly: the design of structure and hierarchy in two and three dimensions *Chem. Rev.* **115** 6265–311

[16] Kinoshita S and Yoshioka S 2005 Structural colors in nature: the role of regularity and irregularity in the structure *ChemPhysChem* **6** 1442–59

[17] Phillips K R *et al* 2016 A colloidoscope of colloid-based porous materials and their uses *Chem. Soc. Rev.* **45** 281–322

[18] Noh H *et al* 2010 How noniridescent colors are generated by quasi-ordered structures of bird feathers *Adv. Mater.* **22** 2871–80

[19] Biró L P and Vigneron J P 2011 Photonic nanoarchitectures in butterflies and beetles: valuable sources for bioinspiration *Laser Photonics Rev.* **5** 27–51

[20] Burresi M *et al* 2014 Bright-white beetle scales optimise multiple scattering of light *Sci. Rep.* **4** 6075

[21] Magkiriadou S, Park J-G, Kim Y-S and Manoharan V N 2012 Disordered packings of core–shell particles with angle-independent structural colors *Opt. Mater. Express* **2** 1343

[22] Magkiriadou S, Park J G, Kim Y S and Manoharan V N 2014 Absence of red structural color in photonic glasses, bird feathers, and certain beetles *Phys. Rev.* E **90** 062302

[23] Takeoka Y *et al* 2013 Production of colored pigments with amorphous arrays of black and white colloidal particles *Angew. Chem., Int. Ed. Engl.* **52** 7261–65

[24] Harun-Ur-Rashid M *et al* 2010 Angle-independent structural color in colloidal amorphous arrays *ChemPhysChem* **11** 579–83

[25] Kumano N, Seki T, Ishii M, Nakamura H and Takeoka Y 2011 Tunable angle-independent structural color from a phase-separated porous gel *Angew. Chem., Int. Ed. Engl.* **50** 4012–5

[26] Ge D *et al* 2015 A robust smart window: reversibly switching from high transparency to angle-independent structural color display *Adv. Mater.* **27** 2489–95

[27] Park J G *et al* 2014 Full-spectrum photonic pigments with non-iridescent structural colors through colloidal assembly *Angew. Chem., Int. Ed. Engl.* **53** 2899–903

[28] Vukusic P, Sambles J R, Lawrence C R and Wootton R J 1999 Quantified interference and diffraction in single Morpho butterfly scales *Proc. R. Soc.* B **266** 1403–11

[29] Wilts B D, Giraldo M A and Stavenga D G 2016 Unique wing scale photonics of male Rajah Brooke's birdwing butterflies *Front. Zool.* **13** 36

[30] Song B, Johansen V E, Sigmund O and Shin J H 2017 Reproducing the hierarchy of disorder for Morpho-inspired, broad-angle color reflection *Sci. Rep.* **7** 46023

[31] Chung K *et al* 2012 Flexible, angle-independent, structural color reflectors inspired by morpho butterfly wings *Adv. Mater.* **24** 2375–9

[32] Schaffner M, England G, Kolle M, Aizenberg J and Vogel A N 2015 Combining bottom-up self-assembly with top-down microfabrication to create hierarchical inverse opals with high structural order *Small* **11** 4334–40

[33] Hsiung B-K *et al* 2017 Tarantula-inspired noniridescent photonics with long-range order *Adv. Opt. Mater.* **5** 1600599

[34] Umh H N, Yu S, Kim Y H, Lee S Y and Yi J 2016 Tuning the structural color of a 2D photonic crystal using a bowl-like nanostructure *ACS Appl. Mater. Interfaces* **8** 15802–8

[35] England G *et al* 2014 Bioinspired micrograting arrays mimicking the reverse color diffraction elements evolved by the butterfly *Pierella luna Proc. Natl Acad. Sci. USA* **111** 15630–4

[36] Vigneron J P *et al* 2010 Reverse color sequence in the diffraction of white light by the wing of the male butterfly *Pierella luna* (Nymphalidae: Satyrinae) *Phys. Rev.* E **82** 021903

[37] Kolle M *et al* 2010 Mimicking the colourful wing scale structure of the *Papilio blumei* butterfly *Nat. Nanotechnol.* **5** 511–5

[38] Ferry V E, Munday J N and Atwater H A 2010 Design considerations for plasmonic photovoltaics *Adv. Mater.* **22** 4794–808

[39] Yu Z, Raman A and Fan S 2010 Fundamental limit of light trapping in grating structures *Opt. Express* **18** A366–80

[40] Leung S F *et al* 2012 Efficient photon capturing with ordered three-dimensional nanowell arrays *Nano Lett.* **12** 3682–9

[41] Raman A, Yu Z and Fan S 2011 Dielectric nanostructures for broadband light trapping in organic solar cells *Opt. Express* **19** 19015–26

[42] Chen J Y *et al* 2014 Enhanced performance of organic thin film solar cells using electrodes with nanoimprinted light-diffraction and light-diffusion structures *ACS Appl. Mater. Interfaces* **6** 6164–9

[43] Zhang R Y, Shao B, Dong J R, Zhang J C and Yang H 2011 Absorption enhancement analysis of crystalline Si thin film solar cells based on broadband antireflection nanocone grating *J. Appl. Phys.* **110** 113105

[44] Yao Y, Liu H and Wu W 2014 Spectrum splitting using multi-layer dielectric meta-surfaces for efficient solar energy harvesting *Appl. Phys.* A **115** 713–9

[45] Meng X *et al* 2012 Combined front and back diffraction gratings for broad band light trapping in thin film solar cell *Opt. Express* **20** A560–71

[46] Hsu C-M *et al* 2012 High-efficiency amorphous silicon solar cell on a periodic nanocone back reflector *Adv. Energy Mater.* **2** 628–33

[47] Moon Y J *et al* 2016 Microstructured air cavities as high-index contrast substrates with strong diffraction for light-emitting diodes *Nano Lett.* **16** 3301–8

[48] Kim J J *et al* 2016 Biologically inspired organic light-emitting diodes *Nano Lett.* **16** 2994–3000

[49] Seo H B and Lee S Y 2017 Bio-inspired colorimetric film based on hygroscopic coloration of longhorn beetles (Tmesisternus isabellae) *Sci. Rep.* **7** 44927

[50] Shawkey M D and Hill G E 2006 Significance of a basal melanin layer to production of non-iridescent structural plumage color: evidence from an amelanotic Steller's jay (Cyanocitta stelleri) *J. Exp. Biol.* **209** 1245–50

[51] Xiao M *et al* 2015 Bio-inspired structural colors produced via self-assembly of synthetic melanin nanoparticles *ACS Nano* **9** 5454–60

[52] Kohri M, Nannichi Y, Taniguchi T and Kishikawa K 2015 Biomimetic non-iridescent structural color materials from polydopamine black particles that mimic melanin granules *J. Mater. Chem.* C **3** 720–4

[53] Zhang Y *et al* 2015 Using cuttlefish ink as an additive to produce -non-iridescent structural colors of high color visibility *Adv. Mater.* **27** 4719–24

[54] Josephson D P, Miller M and Stein A 2014 Inverse opal $SiO_2$ photonic crystals as structurally-colored pigments with additive primary colors *Z. Anorg. Allg. Chem.* **640** 655–62

[55] Pursiainen O L *et al* 2007 Nanoparticle-tuned structural color from polymer opals *Opt. Express* **15** 9553

[56] Aguirre C I, Reguera E and Stein A 2010 Colloidal photonic crystal pigments with low angle dependence *ACS Appl. Mater. Interfaces* **2** 3257–62

[57] Vogel N *et al* 2015 Color from hierarchy: diverse optical properties of micron-sized spherical colloidal assemblies *Proc. Natl Acad. Sci. USA* **112** 10845–50

[58] Koay N *et al* 2014 Hierarchical structural control of visual properties in self-assembled photonic–plasmonic pigments *Opt. Express* **22** 27750–68

[59] Klupp Taylor R N *et al* 2011 Painting by numbers: nanoparticle-based colorants in the post-empirical age *Adv. Mater.* **23** 2554–70

[60] Saito K and Tatsuma T 2015 Asymmetric three-way plasmonic color routers *Adv. Opt. Mater.* **3** 883–7

[61] England G T *et al* 2017 The optical Janus effect: asymmetric structural color reflection materials *Adv. Mater.* **29** 1606876

[62] Saito K and Tatsuma T 2016 Control of asymmetric scattering behavior of plasmonic nanoparticle ensembles *ACS Photonics* **3** 1782–6

[63] Butun S and Aydin K 2015 Asymmetric light absorption and reflection in freestanding nanostructured metallic membranes *ACS Photonics* **2** 1652–7

[64] Jalas D *et al* 2013 What is—and what is not—an optical isolator *Nat. Photon.* **7** 579–82

[65] Ding B, Qiu M and Blaikie R J 2014 Manipulating light absorption in dye-doped dielectric films on reflecting surfaces *Opt. Express* **22** 25965–75

[66] Yu R *et al* 2016 Structural coloring of glass using dewetted nanoparticles and ultrathin films of metals *ACS Photonics* **3** 1194–201

[67] Kats M A *et al* 2012 Ultra-thin perfect absorber employing a tunable phase change material *Appl. Phys. Lett.* **101** 221101

[68] Kats M A *et al* 2013 Enhancement of absorption and color contrast in ultra-thin highly absorbing optical coatings *Appl. Phys. Lett.* **103** 101104

[69] Kats M A, Blanchard R, Genevet P and Capasso F 2013 Nanometre optical coatings based on strong interference effects in highly absorbing media *Nat. Mater.* **12** 20–4

[70] Kats M A and Capasso F 2014 Ultra-thin optical interference coatings on rough and flexible substrates *Appl. Phys. Lett.* **105** 131108

[71] Kats M A, Blanchard R, Ramanathan S and Capasso F 2014 Thin-film interference in lossy, ultra-thin layers *Opt. Photonics News* **25** 40

[72] Mirshafieyan S S and Guo J 2014 Silicon colors: spectral selective perfect light absorption in single layer silicon films on aluminum surface and its thermal tunability *Opt. Express* **22** 31545–54

[73] Cao T, Wei C W, Simpson R E, Zhang L and Cryan M J 2014 Broadband polarization-independent perfect absorber using a phase-change metamaterial at visible frequencies *Sci. Rep.* **4** 3955

[74] Park J *et al* 2014 Omnidirectional near-unity absorption in an ultrathin planar semiconductor layer on a metal substrate *ACS Photonics* **1** 812–21

[75] Ding F, Mo L, Zhu J and He S 2015 Lithography-free, broadband, omnidirectional, and polarization-insensitive thin optical absorber *Appl. Phys. Lett.* **106** 061108

[76] Lee K-T, Lee J Y, Seo S and Guo L J 2014 Colored ultrathin hybrid photovoltaics with high quantum efficiency *Light Sci. Appl.* **3** e215

[77] Lee K-T, Fukuda M, Joglekar S and Guo L J 2015 Colored, see-through perovskite solar cells employing an optical cavity *J. Mater. Chem.* C **3** 5377–82

[78] Diest K, Dionne J A, Spain M and Atwater H A 2009 Tunable color filters based on metal–insulator–metal resonators *Nano Lett.* **9** 2579–83

[79] Xu T, Wu Y K, Luo X and Guo L J 2010 Plasmonic nanoresonators for high-resolution colour filtering and spectral imaging *Nat. Commun.* **1** 1–5

[80] Li Z, Butun S and Aydin K 2015 Large-area, lithography-free super absorbers and color filters at visible frequencies using ultrathin metallic films *ACS Photonics* **2** 183–8

[81] Park C S, Shrestha V R, Lee S S and Choi D Y 2016 Trans-reflective color filters based on a phase compensated etalon enabling adjustable color saturation *Sci. Rep.* **6** 25496

[82] Kwon H and Kim S 2015 Chemically tunable, biocompatible, and cost-effective metal–insulator–metal resonators using silk protein and ultrathin silver films *ACS Photonics* **2** 1675–80

[83] Yang Z *et al* 2016 Reflective color filters and monolithic color printing based on asymmetric Fabry–Perot cavities using nickel as a broadband absorber *Adv. Opt. Mater.* **4** 1196–202

[84] Poddubny A, Iorsh I, Belov P and Kivshar Y 2013 Hyperbolic metamaterials *Nat. Photon.* **7** 948–57

[85] Sreekanth K V *et al* 2016 Extreme sensitivity biosensing platform based on hyperbolic metamaterials *Nat. Mater.* **15** 621–7

[86] Li Z, Clark A W and Cooper J M 2016 Dual color plasmonic pixels create a polarization controlled nano color palette *ACS Nano* **10** 492–8

[87] Duempelmann L, Casari D, Luu-Dinh A, Gallinet B and Novotny L 2015 Color rendering plasmonic aluminum substrates with angular symmetry breaking *ACS Nano* **9** 12383–91

[88] Duempelmann L, Luu-Dinh A, Gallinet B and Novotny L 2016 Four-fold color filter based on plasmonic phase retarder *ACS Photonics* **3** 190–6

[89] Raj Shrestha V, Lee S S, Kim E S and Choi D Y 2015 Polarization-tuned dynamic color filters incorporating a dielectric-loaded aluminum nanowire array *Sci. Rep.* **5** 12450

[90] Honma H, Ishida M, Takahashi K, Sawada K and Fukuhara M 2014 Free-standing aluminium nanowire arrays for high-transmission plasmonic colour filters *Micro Nano Lett.* **9** 891–5

[91] Zheng J, Ye Z-C and Sheng Z-M 2016 Reflective low-sideband plasmonic structural colors *Opt. Mater. Express* **6** 381

[92] Sun N *et al* 2015 Tunable spectral filters based on metallic nanowire gratings *Opt. Mater. Express* **5** 912

[93] Nawrot M, Zinkiewicz L, Wlodarczyk B and Wasylczyk P 2013 Transmission phase gratings fabricated with direct laser writing as color filters in the visible *Opt. Express* **21** 31919–24

[94] Khorasaninejad M, Abedzadeh N, Walia J, Patchett S and Saini S S 2012 Color matrix refractive index sensors using coupled vertical silicon nanowire arrays *Nano Lett.* **12** 4228–34

[95] Seo K *et al* 2011 Multicolored vertical silicon nanowires *Nano Lett.* **11** 1851–6

[96] Park H and Crozier K B 2015 Vertically stacked photodetector devices containing silicon nanowires with engineered absorption spectra *ACS Photonics* **2** 544–9

[97] Soukoulis C M and Wegener M 2011 Past achievements and future challenges in the development of three-dimensional photonic metamaterials *Nat. Photon.* **5** 523–30

[98] Minovich A E *et al* 2015 Functional and nonlinear optical metasurfaces *Laser Photonics Rev.* **9** 195–213

[99] Gu Y, Zhang L, Yang J K, Yeo S P and Qiu C W 2015 Color generation via subwavelength plasmonic nanostructures *Nanoscale* **7** 6409–19

[100] Shaltout A M, Kildishev A V and Shalaev V M 2016 Evolution of photonic metasurfaces: from static to dynamic *J. Opt. Soc. Am.* B **33** 501

[101] Kumar K *et al* 2012 Printing colour at the optical diffraction limit *Nat. Nanotechnol.* **7** 557–61

[102] Xue J *et al* 2015 Scalable, full-colour and controllable chromotropic plasmonic printing *Nat. Commun.* **6** 8906

[103] Wu Y K, Hollowell A E, Zhang C and Guo L J 2013 Angle-insensitive structural colours based on metallic nanocavities and coloured pixels beyond the diffraction limit *Sci. Rep.* **3** 1194

[104] Xiong K *et al* 2016 Plasmonic metasurfaces with conjugated polymers for flexible electronic paper in color *Adv. Mater.* **28** 9956–60

[105] Cheng F, Gao J, Luk T S and Yang X 2015 Structural color printing based on plasmonic metasurfaces of perfect light absorption *Sci. Rep.* **5** 11045

[106] Roberts A S, Pors A, Albrektsen O and Bozhevolnyi S I 2014 Subwavelength plasmonic color printing protected for ambient use *Nano Lett.* **14** 783–87
[107] Tan S J *et al* 2014 Plasmonic color palettes for photorealistic printing with aluminum nanostructures *Nano Lett.* **14** 4023–9
[108] Clausen J S *et al* 2014 Plasmonic metasurfaces for coloration of plastic consumer products *Nano Lett.* **14** 4499–504
[109] Yue W, Gao S, Lee S S, Kim E S and Choi D Y 2016 Subtractive color filters based on a silicon-aluminum hybrid-nanodisk metasurface enabling enhanced color purity *Sci. Rep.* **6** 29756
[110] Miyata M, Hatada H and Takahara J 2016 Full-color subwavelength printing with gap-plasmonic optical antennas *Nano Lett.* **16** 3166–72
[111] Cheng F *et al* 2015 Aluminum plasmonic metamaterials for structural color printing *Opt. Express* **23** 14552–60
[112] Ye X and Qi L 2011 Two-dimensionally patterned nanostructures based on monolayer colloidal crystals: controllable fabrication, assembly, and applications *Nano Today* **6** 608–31
[113] Vogel N, Weiss C K and Landfester K 2012 From soft to hard: the generation of functional and complex colloidal monolayers for nanolithography *Soft Matter* **8** 4044–61
[114] Zhang J, Li Y, Zhang X and Yang B 2010 Colloidal self-assembly meets nanofabrication: from two-dimensional colloidal crystals to nanostructure arrays *Adv. Mater.* **22** 4249–69
[115] Wang L *et al* 2016 Large area plasmonic color palettes with expanded gamut using colloidal self-assembly *ACS Photonics* **3** 627–33
[116] Ohno T *et al* 2016 Hole-size tuning and sensing performance of hexagonal plasmonic nanohole arrays *Opt. Mater. Express* **6** 1594
[117] Bradley L and Zhao Y 2016 Uniform plasmonic response of colloidal Ag Patchy particles prepared by swinging oblique angle deposition *Langmuir* **32** 4969–74
[118] Honold T, Volk K, Rauh A, Fitzgerald J P S and Karg M 2015 Tunable plasmonic surfaces via colloid assembly *J. Mater. Chem.* C **3** 11449–57
[119] Mendes M J, Morawiec S, Simone F, Priolo F and Crupi I 2014 Colloidal plasmonic back reflectors for light trapping in solar cells *Nanoscale* **6** 4796–805
[120] Chen T and Reinhard B M 2016 Assembling color on the nanoscale: multichromatic switchable pixels from plasmonic atoms and molecules *Adv. Mater.* **28** 3522–7
[121] Zhang C *et al* 2016 Printed photonic elements: nanoimprinting and beyond *J. Mater. Chem.* C **4** 5133–53
[122] Franklin D *et al* 2015 Polarization-independent actively tunable colour generation on imprinted plasmonic surfaces *Nat. Commun.* **6** 7337
[123] Olson J *et al* 2016 High chromaticity aluminum plasmonic pixels for active liquid crystal displays *ACS Nano* **10** 1108–17
[124] Song S *et al* 2017 Actively tunable structural color rendering with tensile substrate *Adv. Opt. Mater.* **5** 1600829

**Joanna Aizenberg** pursues multidisciplinary research that includes biomimetics, crystal and colloidal engineering, biooptics and smart materials. She received the BS degree in Chemistry from the Moscow State University, and PhD in Structural Biology from the Weizmann Institute of Science. After spending nearly a decade at Bell Labs, Joanna joined Harvard University, where she is the Amy Smith Berylson Professor of Materials Science, Director of the Kavli Institute for Bionano Science and Technology, and Platform Leader in the Wyss Institute for Biologically Inspired Engineering. Aizenberg is elected to the American Academy of Arts and Sciences, American Philosophical Society, American Association for the Advancement of Science; and she is a Fellow of the APS, MRS and External Member of the Max Planck Society. Joanna's major awards include MRS Medal, Fred Kavli Distinguished Lectureships from ACS and MRS, Harvard's Ledlie Prize, Ronald Breslow Award in Biomimetic Chemistry, and ACS Industrial Innovation Award. She has served at the Board of Directors of the MRS and at the Board on Physics and Astronomy of the National Academies.

**Grant England** was born in Kentucky in 1986. He received a B.E. in Electrical Engineering from Vanderbilt University in 2009, and a MS and PhD from Harvard University in 2012 and 2017, respectively. His PhD research focused primarily on structural color, bio-inspired photonics, and structurally colored materials. Currently, he is employed as a data scientist in the semiconductor device industry.